INNSPUB

Journal of Biodiversity and Environmental Sciences (JBES)
ISSN: 2220-6663 (Print) 2222-3045 (Online)
Vol. 22, No. 3, p. 9-21, 2023
http://www.innspub.net

RESEARCH PAPER OPEN ACCESS

Kinetic studies on malachite green dye adsorption from aqueous solutions by Algae with Chitosan nanocomposite adsorbent: Nanocomposite synthesis and characterization

SP. Manobala[1], S. Amutha[1], E. Pushpalakshmi[1], T. Madhumitha[1], R. Venkateshwari[1], S. Rajaduraipandian[2], G. Annadurai[*1]

[1]*Sri Paramakalyani Centre of Excellence in Environmental Sciences, Manonmaniam Sundaranar University, Alwarkurichi, India*

[2]*Sri Paramakalyani College, Manonmaniam Sundaranar University, Alwarkurichi, India*

Article published on March 10, 2023

Key words: Algae, Chitosan, FTIR, SEM, TGA, DTA, DTG, Malachite green *dye* and Pseudo-second order kinetic studies

Abstract

Water polluted by dyestuffs compounds is a global threat to health and the environment; accordingly, we prepared a green novel sorbent chemical and Physical system from an algae, chitosan and chitosan nanoparticle and impregnated with algae with chitosan nanocomposite for the sorption of Malachite green *dye* from water. The algae with chitosan nanocomposite by a simple method and used as a recyclable and effective adsorbent for the removal of malachite green dye from aqueous solutions. Algae, chitosan, chitosan nanoparticle and algae with chitosan nanocomposite were characterized using different physicochemical methods. The functional groups and chemical compounds found in algae, chitosan, chitosan algae, chitosan nanoparticle, and chitosan nanoparticle with algae were identified using FTIR, SEM, and TGADTA/DTG techniques. The optimal adsorption conditions, different dosages, pH and Temperature the amount of algae with chitosan nanocomposite were determined. At optimized conditions and the batch equilibrium studies more than 99% of the dye was removed. The adsorption process data matched well kinetics showed that the reaction order for dye varied with pseudo-first order and pseudo-second order. Furthermore, the maximum adsorption capacity of the algae with chitosan nanocomposite toward *malachite green* dye reached as high as 15.5mg/g, respectively. Finally, multiple times reusing of algae with chitosan nanocomposite and removing dye from a real wastewater has made it a promising and attractive option for further practical applications.

***Corresponding Author:** G. Annadurai ✉ gannadurai@msuniv.ac.in

Introduction

Industrial and agricultural activities have all produced organic pollutants, radionuclides, metalloids, and hazardous metals that are creating the environment at risk [G.M. Gadd, 2009]. As per the reports, the textile, dyeing, and painting industries require roughly 10,000 different types of commercially - available dyes and 700 tonnes of dyestuffs annually (Robinsson, 2001). There are several methods for eliminating inorganic compounds from aqueous media. A few techniques that exist are ultrasonic irradiation, chlorination, photodegradation, oxidation, membrane separation, coagulation, biodegradation, precipitation, and adsorption (Lawal *et al.,* 2019; Peternel *et al.,* 2007; Kaur Parul *et al.,* 2020; Martínez-Huitle *et al.,* 2018; Elbaraka *et al.,* 2012).

Active carbon has been reported as the most effective adsorbent (Crisafully *et al.,* 2008), but its usage in large-scale water treatment has been constrained due to its high application costs and challenging regeneration processes/methods.

It has been documented that biosorption is able to reduce about 20% and 28% capital and total costs in comparison with conventional methods respectively (Ata, *et al.,* 2000). Organic dyes, such as safranin, eosin, basic and acid fuchsin, crystal violet, congo red, and methylene blue, among others, are major water pollutants that are mostly found in the effluents of the paper and textile industries (Dogan, *et al.*, 2003). Many researchers used the modified and unmodified algae as an adsorbent to remove different dyes, such as Congo red (Iryani, *et al.,* 2018; Niu, *et al.,* 2019; Bentahar, *et al.,* 2017), basic yellow 28 (Aragaw, *et al.,* 2020), basic yellow 2 (Scoziido1ru, *et al.,* 2016), reactive red 120 (Errais, *et al.,* 2011; Errais, *et al.,* 2012; Abidi, *et al.,* 2019), basic red 46 (Karim, *et al.,* 2009), direct yellow 50 (Yavuz, *et al.,* 2006), methylene blue (Bentahar, *et al.,* 2017; Boukhemkhem, *et al.,* 2017), malachite green (Tehrani-Bagha, *et al.,* 2011), crystal violet (Bentahar, *et al.,* 2017; Nandi, *et al.,* 2008), natural annatto (Dias, *et al.,* 2019), violet 5R and acidic blue 25 (Aguiar, *et al.,* 2017).

One of the most extensively used strategies for immobilisation is the use of polymeric matrixes such as alginate, chitosan, and different resins (Zhao *et al.*, 2011; Karim *et al.*, 2012; Khorramabadi *et al.*, 2012; Darvishi Cheshmeh Soltani *et al.*, 2013). Because of its hydrophilicity, biodegradability, non-toxicity, and availability, chitosan is an appropriate natural biopolymer for the immobilisation process (Cestari *et al.*, 2008; Wan Ngah *et al.*, 2011). Chitosan is nature's second most abundant biopolymer (Zhou *et al.*, 2011; Zhu *et al.*, 2011). Furthermore, the chitosan's adsorption capacity for sequestering anionic dyes due to electrostatic attraction between the protonated amine groups on the chitosan and the anionic dyes' sulfonic groups would be beneficial to enhance anionic dye adsorption in conjunction with the immobilised adsorbent (Chang and Juang, 2004; Zhou *et al.*, 2011; Zhu *et al.*, 2011; Darvishi Cheshmeh Soltani *et al.*, 2013). In this study, the capacity of Malachite green dye to adsorb from aqueous solutions using algae and a chitosan nanocomposite as an adsorbent was examined. The effects of dosages, pH, and temperature on the algae treated with chitosan nanocomposite were investigated under kinetic investigation. Malachite green dye adsorptions onto algae with chitosan nanocomposite are evaluated using the adsorption kinetic data to determine the rate-limiting phase. Both the pseudo-first order and pseudo-second order adsorption isotherms were used to construct the experimental data.

Materials and methods

The following chemicals were of analytical grades Chitosan powder, Acetic acid glacial (CH_3COOH) 100% GR (Merck), Sodium Tripolyphosphate ($Na_5O_{10}P_3$), and double distilled water. Analytical grade Malachite green is an organic compound that is used as a dyestuff and controversially as an antimicrobial in aquaculture. Malachite green is traditionally used as a dye for materials such as silk, leather, and paper. IUPAC name - 4-(4-(Dimethylamino-phenyl-phenyl-methylidene)-*N*, *N*-dimethylcyclohexa-2,5-dien-1-iminium chloride and AS Number – 569-54-2 (Chloride salt) was purchased from Merck.

Algae

Brown marine algae known as *P. boeregeseni* were found in the sea of rameswaram in the southern region, close to rameswaram. The deionized water-cleansed marine algae were freeze-dried, ground into powder, and kept at 4°C for later use. When necessary, 20 g of dried, finely ground *P. boeregeseni* was cooked in 100mL of deionized water for 20 minutes at 60°C. The resulting extract was then passed through a Millipore filter (0.45m) and used for additional experiments within a week at 4°C. They will be dried for 48 hours at 40 degrees Celsius before being ball-milled to a precise geometric size. The pulverised peels were then placed in an airtight container, tagged, and packaged.

Preparation of Chitosan Nanoparticles

Chitosans capacity to form hydrogels in the presence of particular polyanions and its high degree of protonation of the amine functionalities serve as the foundation for the ionic gelation method used to create nanoparticles from chitosan. Chitosan forms nanoparticles when it is cross-linked with a substance like sodium tripolyphosphate (TPP), as a result of the opposing charges between the two molecules. The Ionic Gelation Method is the method used to create chitosan nanoparticles. Polyelectrolytes' ability to cross-link in the presence of opposing ions to produce nanoparticles is the basis for ionotropic gelation. Chitosan polysaccharide is dissolved in an aqueous acidic solution in the ionic gelation process to produce the cation of chitosan. The polyanionic tripolyphosphate solution is then continuously stirred while this solution is added.

Chitosan goes through ionic gelation and precipitates to form spherical particles as a result of the complexation between opposing charges (positive/negative). (Muhammad Rafeeq *et al.*, 2010) Chitosan was dissolved in 2% (v/v) acetic acid after being diluted to 1% w in order to generate a solution. Sodium tripolyphosphate (STPP) (1% (w/v)) was used as an ionic cross-linker. Chitosan nanoparticles were produced by sonicating 10mL of chitosan solution at room temperature for an hour with 1mL of STPP.

Synthesis of Algae with chitosan nanocomposite

With constant magnetic stirring at room temperature, 5.0 g of produced chitosan nanoparticles were dissolved in a 1:1 mixture of ethanol and water. The aforesaid reaction mixture was then mixed with 25g of algae powder. The suspension was continuously agitated for two to four hours before being transferred to a sonication bath for four hours. Centrifugation was used to separate the chitosan nanoparticle from the final product for 30 minutes, and it was then dried in a hot air oven at 100°C. Chitosan nanocomposite containing algae was created.

Characterization of Studies

The functional groups of algae with chitosan nanocomposite were located using the FTIR spectra. On a Perkin Instruments FTIR spectrophotometer, samples' IR spectra were captured. A scanning electron microscope (SEM) and energy-dispersive X-ray spectroscopy (EDX) were used with a Merlin Compact 6073 scanning electron microscope to determine the surface morphology, textural structure, and elemental content of the samples (Carl Zeiss, Germany). Ultraviolet-visible (UV-Vis) spectrophotometry, a method for measuring light absorbance across the ultraviolet and visible ranges of the electromagnetic spectrum, was used to quantify the dye concentration. In the thermal analysis technique known as thermogravimetric analysis (TGA), the mass of a sample is tracked over time as the temperature varies.

Adsorption methods

In doubly distilled water, a stock solution of the Malachite green dye (1000ppm) was made. Under a variety of process variables, including pH, time, temperature, and adsorbate concentration, the adsorption of dye was investigated in batch mode studies. The process of dye adsorption involved shaking a known volume of dye solution in a shaker at a constant speed of 180 rpm for a predetermined amount of time, after which the adsorbent was separated by centrifugation. After that, (UV-Vis) spectrophotometry was employed to measure the concentration of dye in the supernatant. 0.1 M HCl and 0.1 M NaOH were used to change the pH of the

mixture. The following equations (1) and Table.1 were used to determine the amount of dye ions adsorbed. q_e (mg/g) is the quantity of dye adsorbed onto the adsorbent at equilibrium, V (L) is the volume of solution, and m (g) is the mass of the adsorbent, where C_o (mg/L) and C_e (mg/L) are the initial and equilibrium concentrations of dye, respectively.

$$q_e = \frac{C_I - C_F}{m} \times v \qquad (1)$$

Table 1. Pseudo-first order and Second-order different types of Linear and Non- Linear form.

Type	Non-linear form	Linear form	Plot
Lagergren Equations Pseudo first order	$q = q_e\left(1-\exp^{-k,t}\right)$	$Log(q_e - q) = \log(q_e) - K_1 t / 2.303$	$Log(q_e - q) vs.t$
Pseudo second order	$q = K_2 q_e t \ / \ 1 + K_2 q_e t$	$t \ / \ q = 1 \ / \ K_2 q_e^{\ 2} + (1 \ / \ q_e)t$	$t \ / \ q.vs.t$

Result and discussions

SEM Analysis

A representative SEM picture of the resulting composites is shown in Fig. 1. The illustration demonstrates the uneven surface and different pore diameters of the algae, chitosan, chitosan algae, chitosan nanoparticle and chitosan nanoparticle algae.

In addition, the morphologies of the chitosan nanoparticles in the algae, chitosan, chitosan algae made of algae do not resemble those of chitosan nanoparticles. The created chitosan nanoparticles with algal exhibit uniform morphological structure and well-developed exterior macroporosity, supporting the successful development of uniform morphologies, as shown in Fig. 1 A and F. Fig. 1 displays SEM pictures of algae, chitosan, chitosan algae, chitosan nanoparticle and chitosan nanoparticle algae.

Although the algal nanoparticles were not filtered and just a little amount of microsize algae were present, they are homogeneous. This size distribution is advantageous because it makes the brown chitosan nanoparticles with algal easier to transport, store, and handle. A microsized fragment of algae can be seen mixed in with the uniform algal nanoparticles in Fig. 1 C and D. Chitosan is described as an efficient algal flocculant by several writers.

Chitosan, a substance with a heterogeneous surface structure, was clearly responsible for this change in the surface (Rashid *et al.*, 2013).

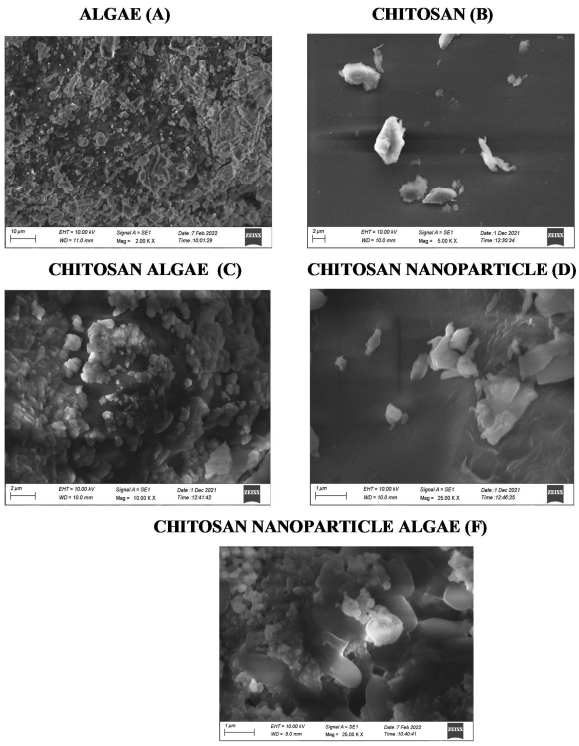

Fig. 1. SEM of the Algae, Chitosan with Algae, Chitosan Nanoparticle, and Chitosan Nanoparticle with Algae Nanocomposite.

Fourier transforms infrared

Fig. 2 displays the findings of the FT-IR study for algae, chitosan, chitosan algae, chitosan nanoparticle, and chitosan nanoparticle. The hydroxyl (-OH) broad peak was seen at about algae (3435cm^{-1}), chitosan (3394cm^{-1}), chitosan algae (3400cm^{-1}), chitosan nanoparticle (3389cm^{-1}), and chitosan nanoparticle algae (3441cm^{-1}) in the FT-IR spectra of algae, chitosan, chitosan algae, and chitosan nanoparticle algae. An absorption peak is seen at 1617cm^{-1}, 1646cm^{-1}, 1741cm^{-1}, 1646cm^{-1}, and 1644cm^{-1},

respectively, in the structures algae, chitosan, chitosan algae, chitosan nanoparticle, and chitosan nanoparticle algae. These absorption peaks can cause tensile vibrations of the C=C groups of unsaturated aliphatic structures and carbonyl/carboxyl structures like C (Song *et al*., 2014; El-Aassar *et al*., 2020; 2021). The vibrations of the C=C group are represented by the absorption peaks at 1420cm^{-1}, 1413cm^{-1}, 1417cm^{-1}, 11385cm^{-1}, and 1385cm^{-1} in the materials algae, chitosan, chitosan algae, chitosan nanoparticle, and chitosan nanoparticle algae. It's also important to note that the vibrations of the functional groups -CO, -OH, and CH are responsible for the vibrations in the ranges of 1038cm^{-1}, 1038cm^{-1}, 1021cm^{-1}, 1038cm^{-1}, 1038cm^{-1}, 1029cm^{-1}, 1094cm^{-1}, and 1073cm^{-1}, respectively. An absorption peak was found in the range of 603-598cm^{-1}in the structure of algae, chitosan, chitosan algae, chitosan nanoparticle, and chitosan nanoparticle algae, which is associated with the bond vibration. According to Fig.s 2, chitosan's peak absorption (amide II and N-H bending vibration) appeared at 1647cm^{-1} and 1644cm^{-1}, respectively, and algae and chitosan shared the same functional group of hydroxyl (OH) stretching vibration, alkane C-H stretching vibration, and C-O stretching vibration from polysaccharide polymers.

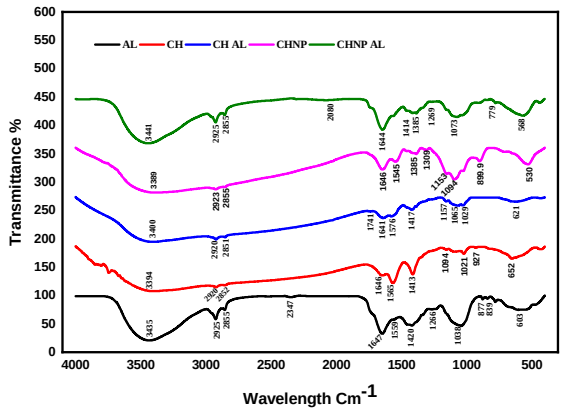

Fig. 2. FTIR curves of the Algae, Chitosan with Algae, Chitosan Nanoparticle, and Chitosan Nanoparticle with Algae Nanocomposite.

Thermal Gravimetric Analysis

The thermal stability behaviour of algae, chitosan, chitosan algae, and chitosan nanoparticle algae was investigated using the TGA analysis. In Fig. 3, the test's outcome is displayed. Up to a temperature of 260°C, weight loss was observed for both samples of algae at a rate of 51.6%, chitosan at a rate of 69%, chitosan algae at a rate of 47.3%, chitosan nanoparticle at a rate of 62.3%, and chitosan nanoparticle algae at a rate of 38.92%. For samples of algae, chitosan, chitosan algae, chitosan nanoparticle, and chitosan nanoparticle algae, the weight loss was discovered to be between 1% and 3% in the first phase, respectively. The evaporation of moisture present in the materials is responsible for the weight loss in the first stage. It is important to note that the weight loss of the chitosan nanoparticle algae sample is more than that of the chitosan, chitosan, chitosan, and algae samples at this stage, which may be caused by the presence of more water molecules in the structure. The breakdown of organic components in the samples and their conversion to gas may be to blame for the second phase of weight loss, which happened in the 220-600°C range. There was a modest weight loss in the samples, which might be the result of the materials under study losing some of their structural integrity. Algae, chitosan, chitosan algae, chitosan nanoparticle, and chitosan nanoparticle algae all commonly lost between 69% and 38.92% of their weight during the TGA procedure. According to the findings, chitosan nanoparticle algae have superior thermal stability than chitosan, algae, chitosan algae, and chitosan nanoparticle. The successful inclusion of algae, chitosan, chitosan algae, chitosan nanoparticles, and chitosan nanoparticle algae structure may be the cause of this stability.

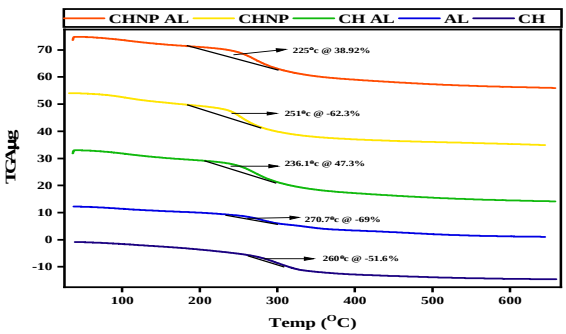

Fig. 3. TGA curves of the Algae, Chitosan with Algae, Chitosan Nanoparticle, and Chitosan Nanoparticle with Algae Nanocomposite.

Differential Thermal Analysis (*DTA/DTG)*

Thermogravimetry and differential thermal analysis have both been used in conjunction for thermal examinations of analytical precipitates. The benefit of using two methods simultaneously is that the same thermal change can be identified and represented by both a weight loss and a temperature change. The findings of the two sets of measurements can be compared in order to spot changes that would not have been obvious without the use of this dual approach. Changes in the sample, whether exothermic or endothermic, can be found relative to the inert reference. Differential thermal analysis was performed using the following materials: algae (293.5 and 471.8°C Wt- 8.83 and 12.32V), chitosan (318.2 and 383.7°C Wt- 147.3 and 67.23V), chitosan algae (293.6 and 544.4°C Wt- 6.070 and 3.314uV), chitosan nanoparticle (112.9.9 and 243.4°C Wt- 126.9 as shown in Fig. 4.

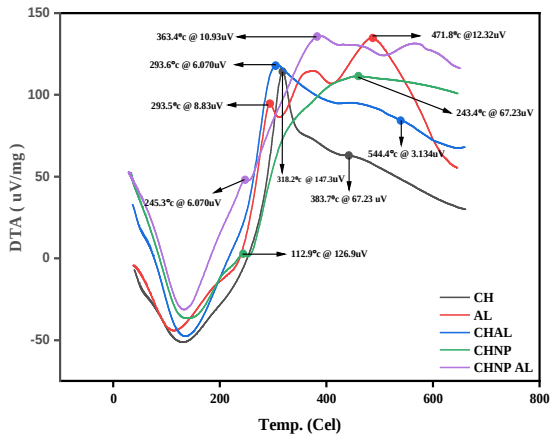

Fig. 4. DTA curves of the Algae, Chitosan with Algae, Chitosan Nanoparticle, and Chitosan Nanoparticle with Algae Nanocomposite.

The differential thermal analysis method also completes the thermogravimetry measurements in the case where there is no weight loss. It is challenging to draw accurate quantitative conclusions from differential thermal analysis thermograms that may be drawn from thermogravimetry results. Similar to the area under a DTA peak study for algae (277°C Wt-5.53mg/min), chitosan (299.6°C Wt-10.63mg/min), chitosan algae (271.3°C Wt-9.19mg/min), chitosan nanoparticle (253°C Wt-10.63mg/min), and chitosan nanoparticle algae (251.6°C Wt-7.69mg/min) as shown in Fig. 5. Then, this differential temperature in algae, chitosan, chitosan algae, chitosan nanoparticle, and chitosan nanoparticle algae is shown against time or against temperature (DTG curve) as shown in Fig. 5.

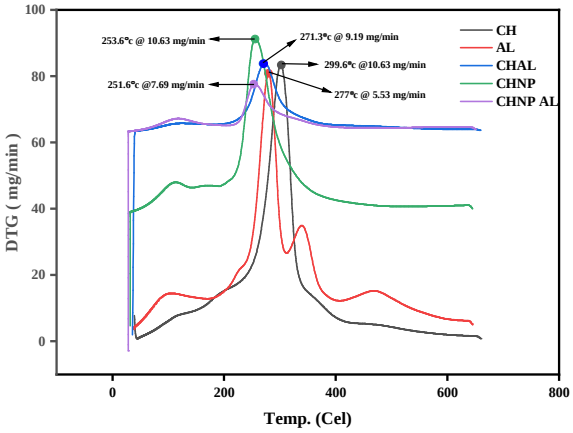

Fig. 5. DTG curves of the Algae, Chitosan with Algae, Chitosan Nanoparticle, and Chitosan Nanoparticle with Algae Nanocomposite.

Effect of dosages

To investigate the influence of algae with chitosan nanocomposite dose on the efficiency and capacity of the adsorption, a test run was done under the conditions of dye concentration of 20mg/L, pH of 8.7, and temperature (30°C) contact time of different min and by orbital shaking instrument. The results are shown in Fig. 6. The same trend was observed for the adsorption process of dye. By increasing the adsorbent dose, the adsorption efficiency of Malachite green dye onto the algae with chitosan nanocomposite increased. This increase in efficiency can be due to an increase in the available surface area to react with dye molecules (Weber *et al.*, 1963; Tehrani-Bagha *et al.*, 2011). According to Fig. 6, with an increase in the adsorbent dose from 20mg/L/100mL to3.0g/100mL, the Malachite green dye adsorption efficiency increased from 75%, respectively. It should be noted that after the dose of 20mg/L/100mL to1.0g/100mL, the adsorption efficiency of cationic dyes using the magnetic composite was not altered. This issue could be due to the adsorbing of approximately all the dye molecules onto the algae with chitosan nanocomposite surface

and the establishment of equilibrium conditions between the pollutant in the solution and on the adsorbent. Also, according to the results, with increasing adsorbent dose, the adsorption capacity of both dyes was reduced (Seozudoru *et al.*, 2016; Sejie and Nadiye, 2016). To justify this, it can be stated that when the algae with chitosan nanocomposite dose in the solution is low, the dye is in contact with all existing active sites on the adsorbent surface and therefore, it becomes adsorbed. In other words, the algae with chitosan nanocomposite surface are saturated with dye molecules. However, by increasing the adsorbent dose in the solution the dye molecule is exposed to active sites that require less energy to adsorb, so it is adsorbed quickly.

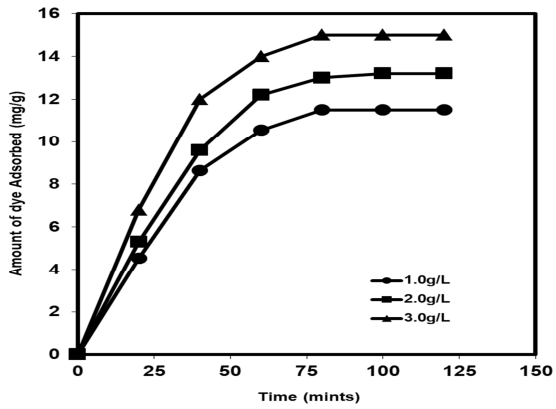

Fig. 6. Effect of specific Malachite green dye uptake at Different Dosages with time (min) algae with chitosan nanocomposite.

Effect of Temperature

The effect of temperature on the sorption of algae with chitosan nanocomposite is shown in Fig 7. The percentage of dye removal decreases from 94% to 89% for dye as the solution temperature increases from 30 to 60°C. Because the adsorption decreased as the temperature increased, the system is considered to be exothermic. A similar trend was reported by (Daneshvar *et al.*, 2007; Dias *et al.*, 2019) for the adsorption of MB on activated carbon prepared from durian shell, who explained that as the temperature increased, the physical bonding between the organic compound (including the dye) and the active sites of the adsorbent weakened. In addition, the dye solubility also increased, which caused the interaction between the solute and solvent to become stronger than that between the solute and adsorbent. Therefore, the solute was more difficult to adsorb in dye molecule.

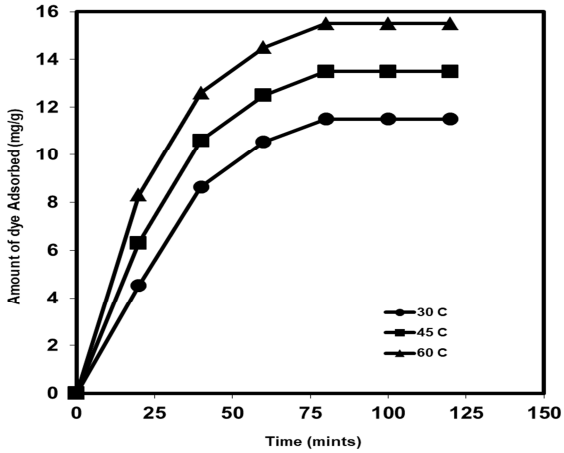

Fig. 7. Effect of specific Malachite green dye uptake at different pH with time (min algae with chitosan nanocomposite.

Effect of pH

Acidity is very important in the adsorption process, especially for dye adsorption. The pH of a medium will control the magnitude of the electrostatic charges imparted by the ionized dye molecules. Both the adsorbent and adsorbate may have functional groups that can be protonated or deprotonated to produce different surface charges in solutions at different pH, resulting in electrostatic attraction or repulsion between the charged adsorbate and adsorbents (Daneshvar *et al.*, 2007; Dias *et al.*, 2019). Therefore, the effect of pH on the adsorption behavior of the dye on the adsorbent was studied by observing the percentage of dye adsorption over a wide pH range of 6.4 to 8.7. The variation in the adsorption of malachite green dye with pH is shown in Fig. 8. As presented in the fig., the obtained results show that the percentage adsorption of dye decreases slightly with increasing basicity up to pH 8.7, after which it remains almost constant. This behavior may be due to the increase in negative charge density of surface at acidic pH, resulting in an attraction between the positively charged dye molecule and adsorbent (Elbaraka *et al.*, 2012; Errais *et al.*, 2011). As the pH increases, the surface charges density on the adsorbent decreases,

resulting in electrostatic repulsion from the positive charge of the dye molecule.

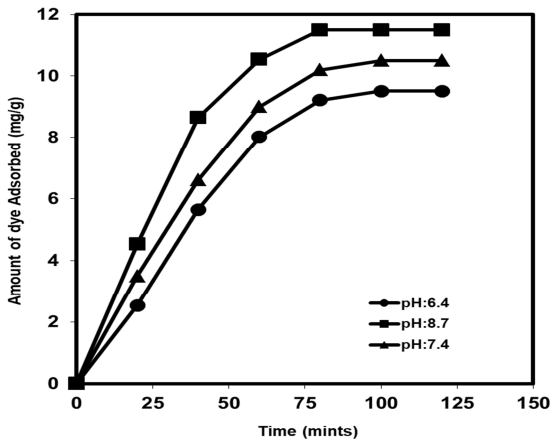

Fig. 8. Effect of specific Malachite green dye - uptake at different temperatures with time (min) algae with chitosan nanocomposite.

Kinetic study

On the basis of kinetic investigations in the adsorption process, the rate and mechanism of adsorption were examined. As a result, several times were chosen for each of the contaminants. According to the suggested method, surface absorption was examined under ideal circumstances using other useful metrics. According to the correlation coefficient values for the linear mode of several kinetic equations, the desired kinetic model was then chosen to explore the kinetics and the mechanism of adsorption. The rate of adsorption is rapid, and the outer surface's adsorption quickly achieves saturation. The dye is simultaneously absorbed by the interior surface of the chitosan nanocomposite particle and enters the algae through a pore within the particle.

The findings of the kinetic experiments are examined using the first-order kinetic model and the second-order kinetic model, respectively, in order to have a thorough understanding of the dye transient behaviour onto algae with chitosan nanocomposite (Hameed *et al.*, 2008). The following equations provide the models. A lumped study of adsorption rates is therefore sufficient for practical operation from the perspective of system design. The pseudo-first-order equation provides a straightforward kinetic analysis of adsorption:

$$\frac{dq_t}{q_t} = K_1\left(q_{eq} - q_t\right) \quad (2)$$

After definite integration by applying the initial conditions q_t=0 at t=0 and q_t=q_t at t=t, equation (2) becomes;

$$\log\left(q_{eq} - q_t\right) = \log q_{eq} - \frac{K_1}{2.303}t \quad (3)$$

Where q_{eq} and q_t are amounts of dye adsorbed at equilibrium and at the time, inmg g-1 respectively, and the k_1 (mg g^{-1} min^{-1}) and q_e (mg g^{-1} min^{-1}), was applied to the present studies of dye adsorption. As such the values of log (q_e-q_t) vs t were calculated from the kinetic data of (Fig. 9 - 11) and plotted against time (Ho and McKay, 1998). The first-order rate constant calculated from the plots is shown in (Table 2).

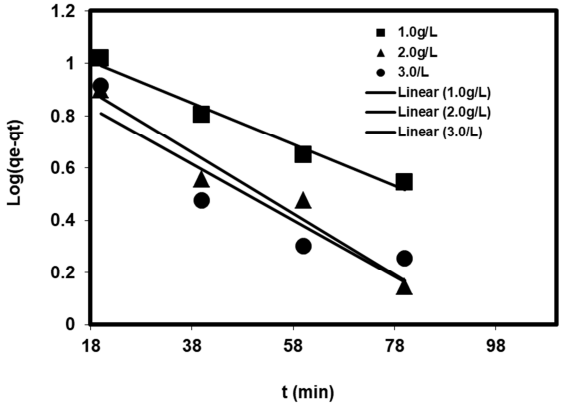

Fig. 9. Pseudo-first order plot for the adsorption of Malachite green dye using algae with chitosan nanocomposite at various plots at Different Dosages.

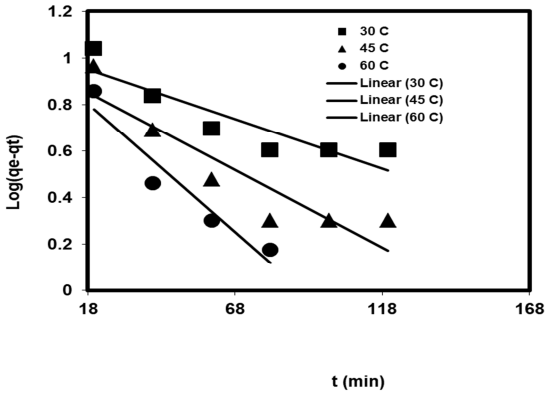

Fig. 10. Pseudo-first order plot for the adsorption of Malachite green dye using algae with chitosan nanocomposite at the various plot at Temperatures.

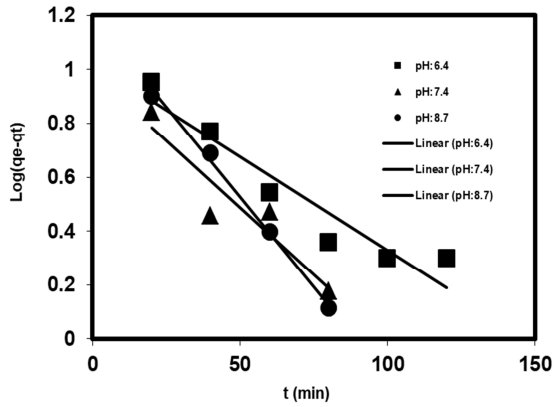

Fig. 11. Pseudo-first order plot for the adsorption of Malachite green dye using algae with chitosan nanocomposite at the various plot at pH.

The Malachite green dye reversible first-order kinetic plot for sorption onto algae with chitosan nanocomposite is shown in Fig. 12-14. Table 3 displays the estimated K values together with the matching R^2 1 values for the linear regression correlation coefficient. The adsorption process' dominance was confirmed by the fact that the forward rate constant K_1 K_2 was significantly higher than the reverse rate constant K_2 (Jumasiah *et al.*, 2005; Konicki *et al.*, 2013). R^2 1 values for the linear regression correlation coefficient were found to vary from 0.8367 to 0.9758, on average, with a value of 0.9944. This model's applicability is confirmed by the lower R^2 1 value; however it is not the right one. The solute sorption onto a sorbent mechanism can be expressed in a number of steps. The constants of sorption and intraparticle diffusion of dyes were calculated using the equations of Lagergren (1898), a pseudo-second order process, and Weber and Morris (1968) in order to explore the sorption mechanism. For some systems, a pseudo-second-order process can also explain adsorption kinetics Franke *et al.* (1987); Bolan *et al.* (1991). The adsorption equilibrium capacity-based pseudo-second-order equation may be written as;

$$\frac{dq_t}{q_t} = K_2 (q_{eq} - q_t)^2 \quad (4)$$

Where k_2 is the rate constant of pseudo-second-order adsorption. Integrating equation (4) and applying the initial conditions, we have

$$\frac{1}{(q_{eq} - q_t)} = \frac{1}{q_e} + K_2 t \quad (5)$$

or equivalently,

$$\frac{t}{q_t} = \frac{1}{K_2 q_{eq}^2} + \frac{1}{q_e} t \quad (6)$$

The equilibrium adsorption capacity (q_{eq}), and the second-order constants k_2 (g/mg min) can be determined experimentally from the slope and intercept of plot t/q_t versus t. The applicability of the pseudo-second-order models can be examined by the linear plot as shown in (Fig. 12-14).

The correlation coefficient R^2 shows that the pseudo-second-order model an indication of chemisorption's mechanism that fits the experimental data slightly better than the pseudo-first-order model. Therefore, the adsorption of Malachite green dye can be approximated more favourably by the pseudo-second-order model (Ho and McKay, 2000; Longhinotti *et al.*, 1998). This model has been successfully applied to describe the kinetics of many adsorption systems. Calculated correlations are closer to unity for the second-order kinetics model; therefore, the adsorption kinetics.

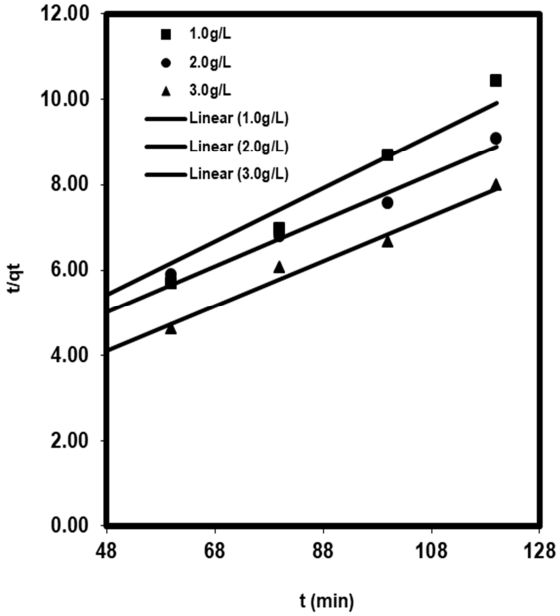

Fig. 12. Pseudo-second order plot for the adsorption of Malachite green dye using algae with chitosan nanocomposite at different Dosages.

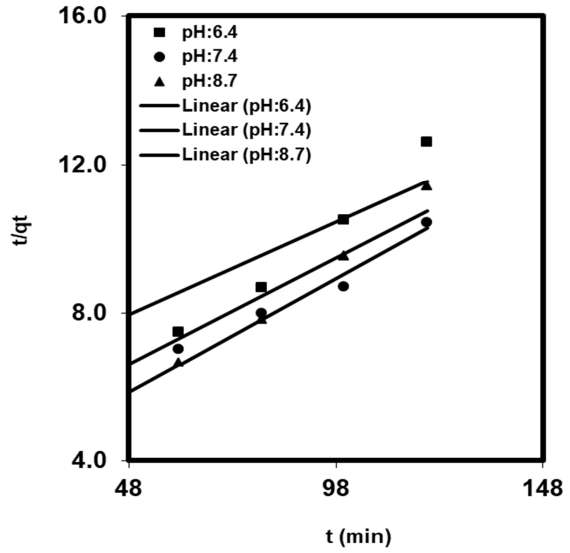

Fig. 13. Pseudo-second order plot for the adsorption of Malachite green dye using algae with chitosan nanocomposite at various plots at pH.

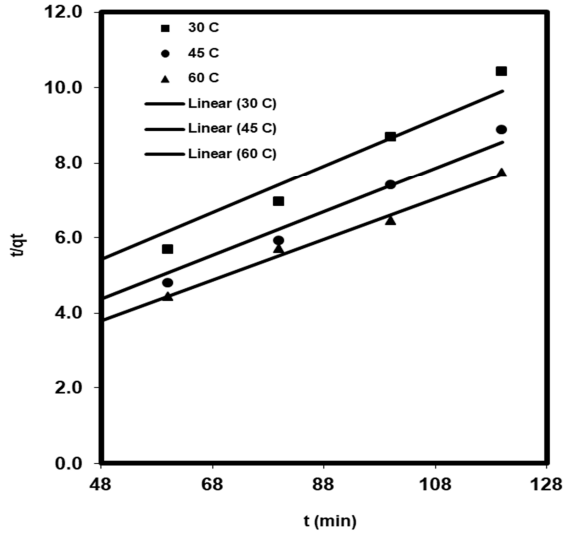

Fig. 14. Pseudo-second order plot for the adsorption of Malachite green dye using algae with chitosan nanocomposite at the various plot at Temperatures.

Table 2. Pseudo-first order rate constant at different dye concentration, pH, and temperature Malachite green dye algae with chitosan nanocomposite.

Pseudo-first order		Pseudo-first-order rate constant
Dosages (g/L)	1.0	K_1=0.0175; q_{eq} =1.149; R^2 = 0.9758
	2.0	K_1=0.0027; q_{eq} =1.103; R^2 = 0.9537
	3.0	K_1=0.0245; q_{eq} =1.0247; R^2 = 0.8556
pH	5.8	K_1=0.0016; q_{eq} =1.417; R^2 = 0.9094
	6.8	K_1=0.0228; q_{eq} =1.540; R^2 = 0.8779
	9.4	K_1=0.0318; q_{eq} =1.459; R^2 = 0.9954
Temperature (°C)	30	K_1=0.009; q_{eq} =1.03; R^2 = 0.8075
	45	K_1=0.0154; q_{eq} =0.971; R^2 = 0.8367
	60	K_1=0.0253; q_{eq} =1.000; R^2 = 0.9234

Table 3. Pseudo second Order (Type - I) rate constant at different dye concentration, pH, and temperature Malachite green dye algae with chitosan nanocomposite.

Pseudo second Order Type - I		Pseudo second order rate constant
Dosages (g/L)	1.0	q_{eq} = 16.07; K_2 = 0.0015; R^2 = 0.9527
	2.0	q_{eq} = 18.55; K_2 = 0.0012; R^2 = 0.9611
	3.0	q_{eq} = 19.04; K_2 = 0.0017; R^2 = 0.9822
pH	5.8	q_{eq} =20.00; K_2 =0.004; R^2 = 0.8062
	6.8	q_{eq} = 17.45; K_2 = 0.008; R^2 = 0.9292
	9.4	q_{eq} = 16.18; K_2 = 0.001; R^2 = 0.9545
Temperature (°C)	30	q_{eq} = 16.07; K_2 = 0.00158; R^2 = 0.9527
	45	q_{eq} = 17.24; K_2 = 0.0021; R^2 = 0.9801
	60	q_{eq} = 18.55; K_2 = 0.0023; R^2 = 0.9944

Conclusion

The kinetics of sorption of Malachite green dye on algae with chitosan nanocomposite was studied on the basis of the pseudo - first - second order rate mechanism. FT-IR, SEM, and TGA were used to determine the morphologies and textural characteristics of the newly synthesised algae with chitosan nanocomposite adsorbent. The sorption of capacity of Malachite green dye is much adsorption Malachite green dye because of the ionic charges on the dye and the character of the composite. Kinetic studies were conducted for dye adsorption on unburned algae with chitosan nanocomposite in aqueous solution. The adsorption of malachite green dye was found to be dependent on solution pH, dosages and temperature were investigated. A comparison of the kinetic models and the overall adsorption capacity was best described by the pseudo first - second-order kinetic model. The activation energy of sorption can be evaluated with the pseudo-second order rate constants. The temperature and pH play a role in the adsorption process. Greater adsorption occurred at high temperature and pH. The thermodynamic calculations indicated that the process was spontaneous and exothermic. The kinetics analysis revealed that the pseudo-second-order model was a better fit of the experimental data than the first-order kinetic expressions. The sorption of malachite green dye by algae with chitosan nanocomposite is an exothermic activated process. For dye/ algae with chitosan nanocomposite systems chemical reaction seems significant in the rate controlling step and also the pseudo-second order

chemical reaction kinetics provide the best correlation of the data. A capacity of sorption has also been evaluated with the pseudo -first - second order rate equation were determined.

References

Abidi NJ, Duplay A, Jada E, Errais M, Ghazi K, Semhi M, Trabelsi A. 2019. Removal of anionic dye from textile industries' effluents by using Tunisian clays as adsorbents. Zeta potential and streaming-induced potential measurements. Compt. Rendus Chem **22,** 113-125.

Aguiar JE, Cecilia PAS, Tavares DCS, Azevedo ER, Castellon SMP, Lucena IJ. 2017. Adsorption study of reactive dyes onto porous clay heterostructures. Appl. Clay Sci **135,** 35 - 44.

Aragaw TA, Angerasa FT. 2020. Synthesis and characterization of Ethiopian kaolin for the removal of basic yellow (BY 28) dye from aqueous solution as a potential adsorbent. Heliyon **6,** 1-16.

Ata A, Nalcaci OO, Ovez B. 2012. Macro algae Gracilaria verrucosa as a biosorbent: a study of sorption mechanisms. Algal Res **1(2),** 194-204.

Bentahar S, Dbik A, El Khomri M, El Messaoudi N, Lacherai A. 2017. Adsorption of methylene blue, crystal violet and Congo red from binary and ternary systems with natural clay: kinetic, isotherm, and thermodynamic. J. Environ. Chem. Eng **5,** 5921- 5932.

Bolan NS, Syers JK, Sumner ME. 1991. Dissolution of various sources of gypsum in aqueous solutions and in soil. J. Sci. Food Agric **57(4),** 527-541

Boukhemkhem A, Rida K. 2017. Improvement adsorption capacity of methylene blue onto modified Tamazert kaolin. Adsorpt. Sci. Technol **35,** 753-777.

Cestari AR, Vieira EFS, Tavares AMG, Bruns RE. 2008. The removal of the indigo carmine dye from aqueous solutions using cross-linked chitosan-eval- uation of adsorption thermodynamics using a full factorial design. Journal of Hazardous Materials **153,** 566-574.

Chang MY, Juang RS. 2004. Adsorption of tannic acid, humic acid, and dyes from water using the composite of chitosan and activated clay. Journal of Colloid and Interface Science **278,** 18-25.

Darvishi Cheshmeh Soltani R, Khataee AR, Safari M, Joo SW. 2013. Preparation of bio-silica/chitosan nanocomposite for adsorption of a textile dye in aqueous solutions. International Biodeterioration & Biodegradation **85,** 383-391

Dias M, Valerio A, de Oliveira D, Ulson de Souza A, de Souza, SMGU. 2019. Adsorption of natural annatto dye by kaolin: kinetic and equilibrium. Environ. Technol **1,** 2648- 2656.

Dogan M, Alkan M. 2003. Adsorption kinetics of methyl violet onto perlite, Chemosphere. **50(4),** 517-528.

Elbaraka N, Saffaj N, Younssi SA, Mamouni R, Laknifli A, Albizane A, Barhon Z. 2012. Photocatalysis-Membrane separation coupling reactor: removal of organic pollutants from water, Scientific Study & Research. Chemistry & Chemical Engineering, Biotechnology. Food Industry **13(1),** 105-108.

Errais E, Duplay J, Darragi F, M'Rabet I, Aubert A, Huber F, Morvan G. Efficient anionic dye adsorption on natural untreated clay: kinetic study and thermodynamic parameter. Desalination **275,** 74- 81.

Errais E, Duplay J, Elhabiri M, Khodja M, Ocampo R, Baltenweck-Guyot R, Darragi F. 2012. Anionic RR120 dye adsorption onto raw clay: surface properties and adsorption mechanism, Colloids Surfaces A Physicochem. Eng. Asp **403,** 69-78.

Franke MD, Ernst WR, Myerson AS. 1987. Kinetics of dissolution of alumina in acidic solution. AIChE Journal **33(2),** 267-273.

Gadd GM. 2009. Biosorption: Critical review of scientific rationale, environmental importance and significance for pollution treatment, J. Chem. Technol. Biotechnol.: International Research in Process. Environmental & Clean Technology **84(1),** 13-28.

Hameed BH, Daud FBM. 2008. Adsorption studies of basic dye on activated carbon derived from agricultural waste: Hevea brasiliensis seed coat. Chemical Engineering Journal **139(1),** 48-55.

Ho Y. 2000. The kinetics of sorption of divalent metal ions onto sphagnum moss peat. Water Research **34(3),** 735-742.

Ho YS, McKay G. 1998. A Comparison of Chemisorption Kinetic Models Applied to Pollutant Removal on Various Sorbents. Process Safety and Environmental Protection **76(4),** 332-340.

Jumasiah A, Chuah TG, Gimbon J, Choong TSY, Azni I. 2005. Adsorption of basic dye onto palm kernel shell activated carbon: sorption equilibrium and kinetics studies. Desalination **186(1-3),** 57-64.

Karim AB, Mounir B, Hachkar M, Bakasse M, Yaacoubi A. 2009. Removal of Basic Red 46 dye from aqueous solution by adsorption onto Moroccan clay, J. Hazard Mater **168,** 304-309.

K**arim Z, Adnan R, Husain Q.** 2012. A b-cyclodextrinechitosan complex as the immobilization matrix for horseradish peroxidase and its application for the removal of azo dyes from textile effluent. International Biodeterioration & Biodegradation **72**, 10-17.

Kaur Parul K, Badru R, Singh PP, Kaushal S. 2020. Photodegradation of organic pollutants using hetero junctions: a review. J. Environ. Chem. Eng **8(2),** 1-66.

Khorramabadi GS, Soltani RDC, Rezaee A, Khataee AR, Jonidi Jafari A. 2012. Utilisation of immobilised activated sludge for the biosorption of chromium (VI). The Canadian Journal of Chemical Engineering **90,** 1539-1546.

Krzysztof C, Xuecheng C, Ewa M, Wojciech K. 2013. Application of hollow mesoporous carbon nanospheres as an high effective adsorbent for the fast removal of acid dyes from aqueous solutions. Chemical Engineering Journal **228,** 824-833.

Lagergren S. 1898. Zur theorie der sogenannten adsorption geloÈster stoffe, Kungliga Svenska Vetenskapsakademiens. Handlingar **24(4),** 1-39.

Longhinotti E, Pozza F, Furlan L, Sanchez M, de N. de M, Klug M, Laranjeira, MCM, Favere VT. 1998. Adsorption of Anionic Dyes on the Biopolymer Chitin. Journal of the Brazilian Chemical Society **9(5),** 435-440.

Martínez-Huitle CAP, anizza M. 2018. Electrochemical oxidation of organic pollutants for wastewater treatment. Current Opinion in Electrochemistry **11,** 62-71.

Mohammed Rafeeq, Ateequrahman, Sanjar Alam, Mikdad. 2016. Automation of plastic, metal and glass waste materials segregation using arduino in scrap industry. International Conference on Communication and Electronics Systems (ICCES).

Nandi BK, Goswami A, Das AK, Mondal B, Purkait MK. 2008. Kinetic and equilibrium studies on the adsorption of crystal violet dye using Kaolin as an adsorbent. Separ. Sci. Technol **43,** 1382-1403.

Niu S, Xie X, Wang Z, Zheng L, Gao F, Miao Y. 2019. Enhanced removal performance for Congo red by coal-series kaolin with acid treatment. Environ. Technol **25,** 1472-1481.

Peternel IT, Koprivanac N, Bozic AML, Kusic HM. 2007. Comparative study of UV/TiO_2, UV/ZnO and photo-Fenton processes for the organic reactive dye degradation in aqueous solution. J. Hazard Mater **148(12),** 477-484.

Rashid N, Rehman MS, Han JI. 2013. Use of chitosan acid solutions to improve separation efficiency for harvesting of the microalga Chlorella vulgaris. Chemical Engineering Journal **226,** 238-242.

Robinson T, McMullan G, Marchant A, Nigam P. 2001. Remediation of dyes in textile effluent: a critical review on current treatment technologies with a proposed alternative. Bioresour. Technol **77(3),** 247-255.

Seozudoru O, Fil BA, Boncukcuollu R, Aladal E, Kul S. 2016. Adsorptive removal of cationic (BY2) dye from aqueous solutions onto Turkish clay: isotherm, kinetic, and thermodynamic analysis. Part, Sci. Technol **34,** 103 -111

Tehrani-Bagha AR, Nikkar H, Mahmoodi NM, Markazi M, Menger FM. 2011. The sorption of cationic dyes onto kaolin: kinetic, isotherm and thermodynamic studies. Desalination **266,** 274-280.

Wan Ngah WS, Teong LC, Hanafiah MAKM. 2011. Adsorption of dyes and heavy metal ions by chitosan composites: a review. Carbohydrate Polymers **83,** 1446-1456.

Weber Jr WJ, Morris JC. 1963. Kinetics of adsorption on carbon from solution, J Sanit Eng Div Am Soc Civ Engrs **89,** 31-59.

Yavuz O, Aydin AH. 2006. Removal of direct dyes from aqueous solution using various adsorbents. Pol. J. Environ. Stud **15,** 155-161.

Zhao X, Lv L, Pan B, Zhang W, Zhang S, Zhang Q. 2011. Polymer-supported nanocomposites for environmental application: A review. Chemical Engineering Journal **170,** 381-394.

Zhou L, Jin J, Liu Z, Liang X, Shang, C. 2011. Adsorption of acid dyes from aqueous solutions by the ethylenediamine-modified magnetic chitosan nano-particles. Journal of Hazardous Materials **185,** 1045-1052.

Zhu HY, Jiang R, Fu YQ, Jiang JH, Xiao L, Zeng GM. 2011. Preparation, characterization and dye adsorption properties of g-Fe_2O_3/SiO_2/chitosan com- posite. Applied Surface Science **258,** 1337-1344.